Mon. Not. R. Astron. Soc. **000**, 000–000 (0000) Printed 19 October 2015 (MN LATEX style file v2.2)

A new method to estimate dark matter halo concentrations

C. Poveda ⋆[1] J. E. Forero-Romero †[1] J. C. Muñoz-Cuartas ‡[2]

[1] *Departamento de Física, Universidad de los Andes, Cra. 1 No. 18A-10, Edificio Ip, Bogotá, Colombia*
[2] *Instituto de Física - FCEN, Universidad de Antioquia, Calle 67 No. 53-108, Medellín, Colombia*

19 October 2015

ABSTRACT

We present a new method to estimate the concentration of dark matter halos in N-body simulations. Our method finds the concentration value to match integrated mass profile as a function of halo radius. The main advantage of this method is that it uses the full particle informatio without any binning. We test our method both on mock and N-body halos to compare it against two popular methods to find concentrations: maximum radial velocity measurements and radial particle binning to estimate the density. Tests on the mock halos show that the accuracy of our method to recover input concentrations varies with the number of particles in the halo. For halos sampled with 20 particles our method recovers the input concentration with 10% accuracy, while for the maximumradial velocity and density methods the accuracy is on the order of 20% and 100%, respectively. For halos with 2×10^4 particles our method achieves an accuracy of 0.01% while the velocity and methods achieve 0.1% and 1%, respectively. We also measure the mass-concentration relationship on N-body data taking care of using halos sampled with at least 200 particles.. We find that at low masses $10^{12}h^{-1}\mathrm{M}_\odot < M < 10^{13}h^{-1}\mathrm{M}_\odot$ our method yields median concentration values lower by a $15\% - 20\%$ compared to the velocity and density methods. At higher masses $3 \times 10^{13}h^{-1}\mathrm{M}_\odot < M < 2 \times 10^{14}h^{-1}\mathrm{M}_\odot$ the three methods give similar results.

Key words: Cosmology: theory - large-scale structure of Universe - Methods: data analysis - numerical - N-body simulations

1 INTRODUCTION

In the concordance cosmological paradigm the matter content of the Universe is dominated by dark matter, a collisionless fluid shaped by gravitational interactions. In the last three decades simulations of dark matter dominated universes have provided valuable insights into the large scale structure formation process, showing a remarkable success in the comparison between theoretical results and observations of the galaxy distribution obtained from surveys. (Springel et al. 2005; Klypin et al. 2011).

On galactic scales the most striking result is that dark matter overdensities closely follow a universal density profile. In a first approximation this profile is spherically symmetric and its density only dependens on the radial coordinate. The universality of this profiles seems to be independent of the cosmological parameters and is self-similar for different spatial scales after an adequate re-scaling is applied. (Navarro et al. 1997; Taylor & Navarro 2001)

One the most popular parameterization for a dark matter halo radial density distribution is the Navarro-Frenk-White (NFW) profile (Navarro et al. 1997). This profile is a double power law in radius, where the transition break happens at the so-called scale radius, r_s. The ratio between the scale radius and the virial radius R_v, which defines a natural scale for the halo, is known as the concentration $c = R_v/r_s$. Simulations also show that the concentration is a strong function of halo mass and redshift.

However, high resolution simulations of Milky Way sized dark matter halos (Navarro et al. 2010) show that the universality property is not perfect and that a better fitting parameterization to the radial density profile is provided by the Einasto profile (Einasto 1965). Nevertheless, the NFW density profile and its concentration have become a standard metric to describe the structure of dark matter halos.

Observationally, the relationship between halo mass and concentration could provide a potential test of the Cold Dark Matter (CDM) paradigm on galactic scales. For this motivation a great deal of effort has been invested in calibrating this relationship with simulations (Neto et al. 2007; Duffy et al. 2008; Muñoz-Cuartas et al. 2011; Prada et al. 2012;

⋆ cn.poveda542@uniandes.edu.co
† je.forero@uniandes.edu.co
‡ xxxx@udea.edu.co

Ludlow et al. 2014) and finding the best possible way to constraint it with observations (Buote et al. 2007; Comerford & Natarajan 2007; Mandelbaum et al. 2008; Giocoli et al. 2014; Foëx et al. 2014; Shan et al. 2015).

In N-body simulations there are two main methods to estimate the concentration parameter of a dark matter halo in a N-body simulation. The first method takes the particles composing the halos and bins them in logarithmic radii to estimate the density in each bin, then it proceeds to fit the density as a function of the radius to the NFW profile. A second method uses an analytic property of the NFW profile that relates the maximum of the ratio of the circular velocity to the virial velocity. The concentration can be then found as the root of a algebraic equation dependent on this maximum value.

The first method is straightforward to apply but presents two disadvantages. First, it requires a large number of particles in order to have a proper density estimate in each bin. This makes the method robust only for halos with at least 10^3 particles. The second problem is that there is not a way to estimate the optimal radial bin size, different choices produce different results for the concentration.

The second method solves the two problems mentioned above. It works with low particles numbers and does not involve data binning. However, it effectively takes into account only a single data point and discards the behaviour of the ratio $V_{\rm circ}/V_{\rm vir}$ below and above its maxima. Additionally, small fluctuations on the value of this maximum can yield large perturbations on the estimated concentration parameter.

In this paper we propose a new method to estimate the dark matter halo concentration in halos from N-body simulations. Our method builds the cumulative mass profile from the particle to find the best possible concentration value fitting this distribution. This proposal has two advantages with respect to the two methods mentioned above. It does not involve any data binning and does not throw away data points.

2 BASIC PROPERTIES OF THE NFW DENSITY PROFILE

Let us review first the basic properties of the NFW density profile. This help us to define our notation and review the important assumptions of the two different methods commonly used to measure the concentration to finally present the new method.

2.1 Density profile

The NFW density profile can be written as

$$\rho(r) = \frac{\rho_c \delta_c}{r/r_s(1+r/r_s)^2}, \tag{1}$$

where $\rho_c \equiv 3H^2/8\pi G$ is the Universe critical density constructed from the Hubble constant H and the universal gravitational constant G, δ_c is the halo dimensionless characteristic density and r_s is the scale radius. This radius marks the transition between the power law scaling $\rho \propto r^{-1}$ for $r < r_s$ and $\rho \propto r^{-3}$ for $r > r_s$.

We define the virial radius of a halo, r_v, as the boundary of the spherical volume that encloses a density of Δ_h times the average density of the Universe. The corresponding mass M_v, the virial mass, can be written as $M_v = \frac{4\pi}{3}\bar{\rho}\Delta_h r_v^3$. From these virial quantities we define new dimensionless variables for the radius and mass $x \equiv r/r_v$ and $m \equiv M(<r)/M_v$.

In this paper we use $\Delta_h = 740$ roughly corresponding to 200 times the critical density.

2.2 Integrated mass profile

From these definitions we can compute the total mass enclosed inside a radius r:

$$M(<r) = 4\pi\rho_c\delta_c r_s^3\left[\ln\left(\frac{r_s+r}{r_s}\right) - \frac{r}{r_s+r}\right], \tag{2}$$

or in terms of the dimensionless mass and radius variables

$$m(<x) = \frac{1}{A}\left[\ln(1+xc) - \left(\frac{xc}{xc+1}\right)\right], \tag{3}$$

where

$$A = \ln(1+c) - \left(\frac{c}{c+1}\right), \tag{4}$$

and the parameter c corresponds to the concentration $c \equiv r_v/r_s$.

From this normalization value and for later convenience we define the following function

$$f(x) = \ln(1+x) - \left(\frac{x}{x+1}\right). \tag{5}$$

The most interesting feature of Eq. (3) is that the concentration is the only free parameter to describe the integrated mass profile.

2.3 Circular velocity profile

It is also customary to express the mass of the halo in terms of the circular velocity $V_c = \sqrt{GM(<r)/r}$. From this we can define a new dimensionless circular velocity $v(<x) \equiv V_c(<r)/V_c(<r_v)$, using the result in Eq. 3 to have:

$$v(<x) = \sqrt{\frac{1}{A}\left[\frac{\ln(1+xc)}{x} - \frac{c}{xc+1}\right]}, \tag{6}$$

This normalized profile always shows a maximum provided that the concentration is larger than $c > 2$. It is possible to show that for the NFW profile the maximum is provided by

$$\max(v(<x)) = \sqrt{\frac{c}{x_{\rm max}}\frac{f(x_{\rm max})}{f(c)}}, \tag{7}$$

where $x_{\rm max} = 2.163$ (Klypin et al. 2014) and the function $f(x)$ was defined in Eq. (5).

3 METHODS TO ESTIMATE THE CONCENTRATION FROM N-BODY SIMULATIONS

3.1 Estimates from the density and velocity profiles

There are two standard methods to estimate concentrations in dark matter halos extracted from N-body simulations.

The first method tries to directly estimate the density profile. It takes all the particles in the halo and bins them in the logarithm of the radial coordinate from the halo center. Then, it estimates the density in each logarithmic bin counting the particles and dividing by the corresponding shell volume. At this point is is possible to make a direct fit to the density as a function of the radial coordinate. This method has been most recently used by Ludlow et al. (2014) to study the mass-concentration-redshift relation of dark matter halos using the Millennium Simulation Series.

A second method uses the circular velocity profile. It finds the value of x for which the normalized circular velocity $v(< x)$ shows a maximum. Using this value it solves numerically for the corresponding value of the concentration using Eq. (7). This method has been most recently used by Klypin et al. (2014) to study the mass-concentration-redshift relation using the Multidark Simulation Suite.

3.2 Our proposal: estimate from the integrated mass profile

Our method uses the integrated mass profile. First we define the center of the halo to be at the position of the particle with the lowest gravitational potential. Then we rank the particles by their increasing radial distance from the center. From this ranked list of $i = 1, N$ particles, the total mass at a radius r_i is $M_i = i \times m_p$, where r_i is the position of the i-th particle and m_p is the mass of a single computational particle. In this process we discard the particle at the center.

We divide the enclosed mass mass M_i and the radii r_i by their virial values to obtain the dimensionless variables m_i and x_i. Once the mass profile is expressed in dimensionless variables the concentration is the only free parameter. We use an Affine Invariant Markov chain Monte Carlo implemented in the python module emcee (Foreman-Mackey et al. 2013) to sample the likelihood function distribution defined by $\mathcal{L}(c) \propto \exp(-\chi^2(c)/2)$ where the $\chi^2(c)$ is written as

$$\chi^2(c) = \sum_{i=1}^{N} [\log m_i - \log m(< x_i; c)]^2, \tag{8}$$

where $m(< x_i; c)$ corresponds to the values in Eq.(3) at $x = x_i$ for a given value of the concentration parameter c and the i index sums over all the particles in the numerical profile. From the χ^2 distribution we find the optimal value of the concentration and its associated uncertainty.

The construction of the numerical integrated mass profile has two advantages with respect to the density and velocity methods, it does not involve any binning (unlike the density methods) and the sampling method uses the information from all the particles in the halo (unlike the velocity method).

4 RESULTS

We now present the results of applying the three methods above mentione on two different halo samples. The first sample is composed by mock halos generated to have known concentration values in perfect spherical symmetry following an NFW profile. We use this sample to check that we can recover the expected values but also gauge the impact of the number of particles on the outcomes. The second sample comes from a publicly available N-body cosmological simulation. From this sample we quantify again the differences between all the methods and also estimate the impact on the mass-concentration relationship.

4.1 Mock halo sample

The method we use to generate the mock halos is based on the integrated mass profile. We start by fixing the desired concentration c and total number of particles N in the mock halo. With these values we define the mass element as $\delta m = 1/M$, corresponding to the mass of each particle such that the total mass is one. Then for each particle, $i = 1, \ldots, N$, we find the value of r_i such that the difference

$$m(< r_i; c) - i \cdot \delta m \tag{9}$$

is zero using Ridders' method.

The value of r_i is the radius of the i-th particle of the mock halo. Then we generate random polar and azimuthal angles θ and ϕ for each particle to ensure spherical symmetry. Finally these three spherical coordinates are transformed into Cartesian coordinates $(r, \theta, \phi) \rightarrow (x, y, z)$.

We generate in total 400 mock halos split into four different groups of 100 halos each. The four groups differ in the total number of particles for their halos: 20, 200, 2000 and 20000. Inside each group the halos have random concentration values in the range $1 < c < 20$ with a uniform distribution. For all these halos ww the concentration values using the density, velocity and mass methods described in the previous section. We quantify the difference between the expected c_{in} and obtained c_{out} values by

$$D = (c_{in} - c_{out})/c_{in}, \tag{10}$$

and

$$\langle |D| \rangle = \frac{1}{|\mathcal{H}|} \sum_{\mathcal{H}} |D|, \tag{11}$$

where $\mathcal{H}$ corresponds to a set of mock halos, and $|\mathcal{H}|$ is the number of haloes in $\mathcal{H}$.

Figure 1 shows the behaviour of $\langle |D| \rangle$ as a function of halo particle number for the three different methods to estimate the concentration.

At fixed particle numbers our method always shows the lowest $\langle |D| \rangle$ values compared to the other two methods. Its accuracy is on the order of 10% for 20 particles in the halo, going down to 0.01% for halos with 20000 particles. The dependence of $\langle |D| \rangle$ with the particle number N goes approximately as $\langle |D| \rangle \propto N^{-1/2}$, hinting that the accuracy of the method is related to a decrease of Poisson noise.

The method based on the maximum of the circular velocity shows a similar behaviour $\langle |D| \rangle \propto N^{-1/2}$. Its accuracy is $2 - 5$ times less than in our method, on the order of 20% for 20 particle halos and 0.5% for 20000 particle halos.

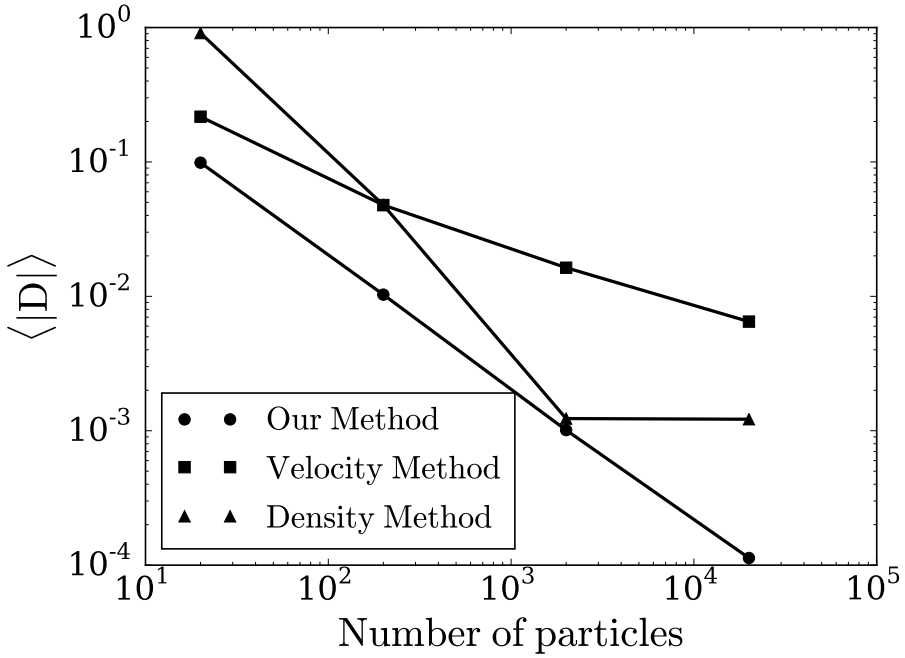

Figure 1. Average value of the relative error in the concentration estimate, $\langle |D| \rangle$, as a function of the particle number N in the set of mock halos. Different symbols represent different methods. Our method provide the most accurate estimate at fixed particle number N.

The method based on the direct density fit shows the lowest accuracy for a low particle number and an intermediate accuracy between the other two methods for a high particle number.

4.2 Halos from a cosmological simulation

REFERENCES

Buote D. A., Gastaldello F., Humphrey P. J., Zappacosta L., Bullock J. S., Brighenti F., Mathews W. G., 2007, ApJ, 664, 123

Comerford J. M., Natarajan P., 2007, MNRAS, 379, 190

Duffy A. R., Schaye J., Kay S. T., Dalla Vecchia C., 2008, MNRAS, 390, L64

Einasto J., 1965, Trudy Astrofizicheskogo Instituta Alma-Ata, 5, 87

Foëx G., Motta V., Jullo E., Limousin M., Verdugo T., 2014, A&A, 572, A19

Foreman-Mackey D., Hogg D. W., Lang D., Goodman J., 2013, PASP, 125, 306

Giocoli C., Meneghetti M., Metcalf R. B., Ettori S., Moscardini L., 2014, MNRAS, 440, 1899

Klypin A., Yepes G., Gottlober S., Prada F., Hess S., 2014, ArXiv e-prints

Klypin A. A., Trujillo-Gomez S., Primack J., 2011, ApJ, 740, 102

Ludlow A. D., Navarro J. F., Angulo R. E., Boylan-Kolchin M., Springel V., Frenk C., White S. D. M., 2014, MNRAS, 441, 378

Mandelbaum R., Seljak U., Hirata C. M., 2008, JCAP, 8, 6

Muñoz-Cuartas J. C., Macciò A. V., Gottlöber S., Dutton A. A., 2011, MNRAS, 411, 584

Navarro J. F., Frenk C. S., White S. D. M., 1997, ApJ, 490, 493

Navarro J. F., Ludlow A., Springel V., Wang J., Vogelsberger M., White S. D. M., Jenkins A., Frenk C. S., Helmi A., 2010, MNRAS, 402, 21

Neto A. F., Gao L., Bett P., Cole S., Navarro J. F., Frenk C. S., White S. D. M., Springel V., Jenkins A., 2007, MNRAS, 381, 1450

Prada F., Klypin A. A., Cuesta A. J., Betancort-Rijo J. E., Primack J., 2012, MNRAS, 423, 3018

Shan H., Kneib J.-P., Li R., Comparat J., Erben T., Makler M., Moraes B., Van Waerbeke L., Taylor J. E., Charbonnier A., 2015, ArXiv e-prints

Springel V., White S. D. M., Jenkins A., Frenk C. S., Yoshida N., Gao L., Navarro J., Thacker R., Croton D., Helly J., Peacock J. A., Cole S., Thomas P., Couchman H., Evrard A., Colberg J., Pearce F., 2005, Nature, 435, 629

Taylor J. E., Navarro J. F., 2001, ApJ, 563, 483